Thermal, Electrical Conductivity and CTE Of CF Reinforced Al Composites Fabricated By Hot Compaction

Mostafa Eid, Saleh Kayetbay, Omayma Elkady, Ahmed El-Assal

Abstract— Powder metallurgy technique was used to develop carbon fiber reinforced aluminium composites. By enhancing the wettability between CF and Al matrix through surface coating with a thin layer of nano Cu by the electroless plating technique. Two series of samples are prepared from 0,5,10,15 wt% CF/Al composites. For comparison, one of them was prepared from uncoated sample CF and the other group from Cu-coated ones. Both groups are fabricated by a uniaxial hot-pressing technique under 700 MPa and 500℃. The effects of reinforcement weight fraction and reinforcement coating on microstructure, density, electrical resistivity, thermal conductivity and coefficient of thermal expansion were studied. The results revealed that the density and CTE were decreased while both electrical and thermal conductivities were improved by increasing CF percent. Harmful $AL4C3$ was absent in all produced composites and no intermediate compounds were detected in coated composites. The Cu coating process was an effective way to improve the interfacial structure. The values of electrical and thermal conductivities of coated composites were higher than those of the uncoated composites, and CTE was reduced to 11.98 k^ (-1) at 15 wt.% Cu-coated CF/Al composite, which is suitable for semiconductor in electronic packaging applications...

Index Terms— Carbon Fiber, Aluminium composites, Powder metallurgy, Surface modifications, Thermal conductivity, Coefficient of thermal expansion, Thermal conductivity

—————————— ◆ ——————————

1. INTRODUCTION

The continuous miniaturization of super calculating speed electronic devices leads to more heat generation through the component. Although traditional materials such as Cu and Al have high thermal conductivity (TC), it is challenging to employ these materials in electronic packages due to their high CTE values [1–3]. For optimum electronic packaging materials, CTE value should fall within the range of ceramic materials to reduce induced thermal stress [4–7]. Currently, thermal management materials with superb TC and low coefficient of thermal expansion (CTE) are developed, and thermal management is applied to ensure reliability and avoid failure due to overheating [8–10]. Metal matrix composites have replaced monolithic metals in thermal management devices to cope with electronic devices requirements [11,12].
Carbon-reinforced metal matrix composites are commonly used in thermal management applications [13,14]. Among these composites are CF/Al composites with superior TC, low CTE, low cost and available composites that have proved to be an excellent heat sink material [15–18]. Silivian,Veillere and Lu [19] concluded that with 50 % CF, TC and CTE of CF/Al composites were 258 W/m.K and 7 k^(-1) , respectively, which is satisfied with the electronic devices' applications.
However, excellent thermal properties for CF/Al composites, low wettability and high reactivity to chemical reactions are the main problems that hinder the development of these composites [20–22]. Briefly, at low processing temperature, the contact angle between Al and carbon is 140°, which prevents the good connected interface, resulting in the creation of pores and voids at the interface [23–25]. Additionally, Al reacts with

carbon at high temperatures and forms the undesirable needle shape of Al4C3 at the interface which deteriorates the thermal properties of composites [15,26]. Al4C3 is produced at the temperatures above 500 ℃ [27–29]. Baker and Bonfield [30] stated that Al4C3 was formed below this temperature and increased with increasing temperature. Consequently, the manufacturing process for CF/Al composites must be controlled to produce functional material with high thermal properties [31,32].
Surface coating and addition alloying elements such as Mg have been reported to enhance the wettability issues [33,34]. However, the alloying elements method is not desirable because the overall properties of composites were altered due to the modification in the matrix composition. Moreover, some alloying element may cause the formation of undesirable phases [25,32]. The electroless coating technique is an autocatalytic process that can produce a uniform coating layer without needing for electricity [35,36]. CF is usually electroless coated with Cu [37–39], Ni [20,40,41]. Cu is a metal with high TC (Cu, k=400 W/m. K) [42]. Moreover, the contact angle between Cu-coated CF and Al is 58° that indicates Al easily wetted to Cu-coated CF [43]. When the electroless Cu coating is applied to CF, the bonding at the interface of CF /Al composites fabricated by vacuum pressure infiltration was improved, and the TC of composites increased from 117 W/m. K to 208 W/m. K [44]. Solid-state methods (e.g., Powder metallurgy) are usually used instead of other conventional liquid processes to avoid excessive detrimental reactions and formation (Al4C3). In this regard, the hot-pressing method is preferred since it occurred at high compaction pressure with relatively low processing temperature (below its melting point of matrix composition) and fully dense shapes can be controlled [45–48]. Many investigations focused on the effect of electroless Cu coating on the mechanical properties of

---

Mostafa Eid, Saleh Kayetbay, and Ahmed El-Assal from Benha Faculty of Engineering, Benha, Egypt
Omayma Elkady from Powder Metallurgy Division, Manufacturing Department, Central Metallurgical Research and Development and Institute, Egypt
Mostafa Eid corresponding author e-mail is
mostafa.abdelmaboud@bhit.bu.edu.eg

CF/Al composites produced by powder metallurgy techniques [49,50]. However, this effect on thermal and electrical properties has not yet studied. So, in this study, a new electroless of nano Cu coating method is introduced to show the effect of surface modification and weight fractions of CF on the microstructure, electrical and thermal properties of composites which prepared by high energy ball milling followed by hot compaction.

2 EXPERIMENTAL PROCEDURES

2.1 Materials
Al powder was used as a composite matrix, and high purity milled CF with diameter of 7μm and a length of 100 μm which purchased from Easy Composites Ltd was used as reinforcement.

2.2 ELECTROLESS COPPER COATING
Before electroless Cu plating, 10 g of CF was firstly sensitized in 350 ml sodium hydroxide solution and stirred at 400 rpm for 15 min. Secondly, the sensitized CF was activated with $AgNO_3$ solution, consisting of 3g/L $AgNO_3$ and 300 ml/L formaldehyde and then stirred at room temperature for 15 min. Nano silver metal was used to facilitate the deposition of nano Cu process on CF surface. Finally, activated CF was immersed in a Cu bath, containing 35 g/L $CuSO_4.5H_2O$, 50 g/L NaOH and 170 g/L $KNaC_4.H_4O_6.4H_2O$. When the solution temperature reached 35 ℃, and pH was adjusted at 13, 200 ml/L formaldehyde was added dropwisely to initiate the reaction. After each step, CF was washed with acetone and distilled water, filtered and dried in the oven at 90 ℃. The coated CF was heated at 450℃ for 2hr under a hydrogen atmosphere to get rid of oxidized Cu.

2.3 MANUFACTURING THE COMPOSITES
In this study, (0,5,10,15) wt. % of uncoated or Cu coated CF were mixed with Al powder in 500 ml steel jars using planetary ball milling (PQ-N2 Planetary Ball Mill) at 250 rpm. The mixed powders were poured into a heat-treated stainless-steel mold. After that, the mold was heated in a muffle furnace at 500 ℃ for 30 min. The mold was then rapidly transferred to 30-ton a uniaxial press, and the mixed powders were compacted at 700 MPa for 10 sec. Finally, the samples were naturally cooled in the air to produce 12mm diameter and 6 mm thickness cylindrical samples. 0.5 wt.% paraffin wax was added to the mixture as a lubricant to ease the sample rejection from the die.

2.4 COMPOSITE CHARACTERIZATION
Samples are prepared for the examination by grounding by using 600-2000 SiC papers, then polished with 3 μm alumina and diamond paste. The morphology and microstructure of powders and bulk samples were observed by both optical microscope and field emission scanning electron microscope (FE-SEM; QUANTAFEG250, Holland). X-ray diffraction (XRD) (model x, pert PRO PANalytical) with Cu k_α radiation was also used to investigate the phase composition of powders and composites. Also, to check any new phases formed during the sintering process
The density of composites was determined by Archimedes'

principle, with distilled water as the suspending medium and compared with the theoretical one according to the rule of mixture to calculate the relative density.
The electrical conductivity of samples was calculated at room temperature using (Material Tester for Metals, PCE-COM 20). Samples with a diameter of 12 mm and a thickness of 4 mm were used for the electrical conductivity test.
Wiedemann-Franz Law in equation 1 is used to measure the TC of composites based on electrical measurements.

$$k=\sigma LT \tag{1}$$

Where k is the thermal conductivity (W/m. K), σ is electrical conductivity (S/m), T is the temperature in Kelvin and L is the Lorenz number, equals to 2.45×10^{-8} $((W.\Omega)/(K^2))$.
The CTE of samples was measured using a differential dilatometer (NETZSCH DIL,402 PC) at temperature ranged between room temperature and 350 ℃ with heating rate 5 ℃/min under argon atmosphere. Equation 2 is used to calculate the mean linear coefficient of thermal expansion (CTE):

$$CTE=\Delta L/(L_0 \times \Delta T) \tag{2}$$

Where CTE is the mean linear coefficient of thermal expansion (k^{-1}), ΔL is a thermal strain (mm), L_0 is the original length (mm), ΔT is the temperature difference between tested and room temperature (K).

3. RESULTS AND DISCUSSION

3.1 POWDERS CHARACTERIZATION
Figure1a shows SEM micrographs of Al powders which have an irregular flattened shape with an average particle size of 60μm±10. While figure 1 b-d presents the as-received, activated and coated CF, respectively. It is observed that CF possesses a smooth surface and circular shape. After the activation process, the fibers keep their original form and silver is homogeneously deposited on the fiber surface. On the other side, CF is fully covered and encapsulated with the Cu layer. Figure 1 e is the EDAX analysis of pure Al that corresponds to the sharp peak of Al element and a small peak of oxygen that may be introduced during the milling process due to the high surface area and high reactivity of Al particles that reacts with oxygen. The results of EDAX of activated and coated CF indicate the presence of Cu, Ag, C without any contamination as shown in figure 1f and g.

3.2 COMPOSITES CHARACTERIZATION AND XRD
Figure 2 shows the SEM micrographs of composites and pure Al, which a and b represents the uncoated CF samples, while c and d images belong to the coated CF ones The Al matrix appears as a light grey area, the CF is the black spots, and the Cu is the white one. No visible pores or fiber degradation are observed in all samples. Most of the reinforcement is broken into smaller dimensions during the milling process and uniformly distributes all over the matrix in (X-Y plane) due to a uniaxial pressing effect and good milling conditions [51]. Cu particles are dispersed in the Al matrix, between CF and Al-CF interface, contributing to the reduction of porosity and

123

agglomerations in coated samples. The elemental EDAX analysis was performed for 10 wt. % CF /Al composites to analyze the sample composition of samples before and after the electroless coating process. As a comparison between the two analysis, it is proved that the precipitation of nano silver and Cu on the CF surface was successfully performed. To examine the interface of the composite, images of samples with a higher magnification are shown in figure 3. It can be observed that there are debonding and low wettability between Al and uncoated CF samples due to the ceramic nature of CF. Many interfacial defects (pores and agglomerations) are formed at the interface. In terms of coated composites, CF well bonded to the Al matrix, and no pores could be detected at the interface due to the capsulation of CF with a metallic nano Cu. The improvement in the interfacial structure had an essential rule in thermal properties of composites, as will be seen later. According to Scherrer's equation results, as shown in Table 1, the crystallite size of CF/Al composites is reduced with an increase in CF content. More reduction is obtained when coated reinforcement is used. Incorporation of CF and metallic coating element into the Al matrix acts as a barrier for dislocation movement of Al, thus grain refinement have occurred during the consolidation process. Figure 4 a and b shows the XRD pattern of the original Al powders and coated CF, respectively. For Al powders, major peaks are appeared at (38.42°) (111), (44.6°) (200), (65.0°) (220), (78.13°) (311) and (82.35°) (222) are detected. While the results of the fiber after coating consists of three primary materials: CF, Cu and Ag. Moreover, one peak corresponds to Cu_2O formed during the coating process. The XRD results of composites revealed that the presence of peaks of Al as a major element with a small peak of CF. CF is marginally observed at a higher percentage of the reinforcement. Neither Cu nor intermediate phase (Al_2Cu) was detected in coated samples due to a small percentage of Cu used in the electroless coating process. What's more, Al_4C_3 was not detected in all produced samples, indicating no reaction occurred between Al and C. This may be due to the hot-pressing consolidation technique, in which the traditional sintering process by a slow heating rate gives a chance for Al_4C_3 to be formed.

3.3 DENSITY RESULTS
Figure 5 indicates the relative density of samples which decrease with increasing the weight percentage of the reinforcement. For instance, relative density is reduced by 4.7% and 3.4 % when 15 wt.% uncoated and coated CF were added to the Al matrix. This may be attributed to the low density of reinforcement material ($1.8 g/cm^3$) as compared to Al ($2.7 g/cm^3$). Additionally, it is known that the compressive strength of CF is higher than Al, so the higher amount of CF causes an increase in the yield pressure of the composites and gradually reduces the densification rate. It is also evident that the Cu-coated samples have higher densification than the uncoated ones, particularly for composites, containing 15 wt.% of CF. These results are related to the enhancement in interfacial bonding and fewer interfacial defects (voids) formed in coated composites (see figure 3), which improved the sintered density of composites. Coating the CF with Cu that has a higher density than Al ($8.9/cm^3$) increases the density value.

3.4 ELECTRICAL RESISTIVITY
Figure 6 presents the effect of CF and electroless Cu coating on the electrical resistivity of CF/Al composites. The electrical resistivity of composites decreases by increasing the CF content. The pure sample has an electrical resistivity of 4.8×10^{-8} Ω·m which changed to 3.8×10^{-8} Ω·m with addition 15 wt.%CF. This improvement in the electrical conductivity may be attributed to the high electrical

conductivity of CF, homogeneous dispersion of reinforcement in the Al and the absence of any harmful reactions at the interface. The presence of conductive reinforcement that is uniformly distributed in the Al matrix enhances the conductive paths for electron transport in materials when it is subject to an electrical charge. Intermediate phases in microstructure are obstacles for the electronic motion [52]. Moreover, in this study, most of the reinforcement located along grain boundaries (see figure 3), increasing the electrical performance of composites [53]. Coated composites have lower electrical resistivity than those of the uncoated ones. Electrical resistivity is reduced by 5.64%,2.2% and 1.3% at 5,10 and 15 wt.%CF, respectively. Well-bonded interface and less agglomeration which are found in coated composites are the keys for electrical conductivity improvement. Low interfacial bonding and agglomeration could restrict and scatter electrons motion and thus, increased electrical resistivity of the composite [54,55].

3.5 THERMAL CONDUCTIVITY (TC)
Figure 7 shows the TC of the uncoated and Cu-coated composites with different weight fractions of reinforcement. The effect of CF on the TC of composites was positive, in which it rises from 152.5 W.m^ (-1). k^ (-1) for the pure sample to 192.9 W.m^ (-1). k^ (-1) and 195.5 W.m^(-1). k^ (-1) for 15 wt.%CF for uncoated and coated CF composites, respectively. Improving TC with an increase in CF content is due to the high TC of CF. Moreover, TC of Cu-coated CF/Al composites is slightly higher than that of uncoated ones. For instance, the percentage of improvement was 6%,2.2%and1.3% for 5,10 and 15 wt.%CF, respectively. This may be due to the good microstructure of the prepared composites, especially the structure of the interface, which is considered one of the most critical factors that affects TC properties [56,57]. The weak bonding and porosity formed in the uncoated structure increase thermal interfacial resistance and reduce the TC of composites. Previous works proved improvement in TC of CF metal composites using electroless Cu coating [10,58,59]. Without Cu coating, there is high surface energy at the interfacial area between Al and CF. Thus, some agglomeration takes place, which comes to the creation of pores that decreases the conductivity because the conductivity of pores is zero [60].

3.6 COEFFICIENT OF THERMAL EXPANSION
Figure 8 demonstrates the CTE of the prepared composites against temperatures ranging from 100-350℃. The CTE of composites increases linearly with increasing temperature. This phenomenon is due to the residual thermal stress generated during the fabrication process. This residual stress exhibited tensile stress on the Al and compressive stress on CF. During the heating process, tensile stress on Al begins to relieve; thus, the matrix starts to expand [61]. On the other side, it is challenging to predict CTE of Al/CF because it depends on many factors such as volume fraction, morphology and size of the reinforcement. So, we an attempt to use the ROM model [62] (equation 3) and turner model [63] (equation 4) to estimate CTE of Al/CF composites.

$$\alpha = \alpha_m V_m + \alpha_r V_r \qquad (3)$$

Where α is coefficient of thermal expansion, V the is volume fraction, and the subscripts m and r denote to matrix and reinforcement, respectively.

$$\alpha = (\alpha_m V_m K_m + \alpha_r V_r K_r)/(V_m K_m + V_r K_r) \qquad (4)$$

Where K_m is the bulk modulus of matrix and K_r
Figure 9 shows a comparison between predicted and experimental

CTE of Al composites. The CTE of pure Al is higher (24.21×10^{-6} k^{-1})) as compared with 13.78×10^{-6} k^{-1} and 11.98×10^{-6} k^{-1} for 15 wt.%CF of uncoated and coated composites, respectively. Such intensive reduction is considered as the result of the mechanical restriction of CF on Al matrix expansion [64]. The CTE values of Cu-coated CF composites are lower than the uncoated ones. The interface is considered a significant factor that affects Al composites thermal expansion [65]. So, the higher bonding strength between CF and Al at interface means the higher ability of CF to restrict expansion of Al. Furthermore, the experimental CTE of composites is lower than the theoretical ones. During milling and compaction process, CF is broken into smaller particles with different size, enlarging in specific surface area of reinforcement,

which increases direct contact areas between Al and CF and tends to reduce the expansion process. Jia et al. [61] stated the reasons for the relative reduction of CTE of experimental than theoretical are porosity and a different size of reinforcement. It is also shown that the CTE of the turner model lying close to measured CTE as compared with the ROM model. This is because the turner model takes into consideration the elastic constant, which represents the mechanical interaction between different material in composites. Generally, the addition of CF either coated or uncoated to the Al matrix decreases the CTE. This is due to the low thermal expansion of CF, due to its ceramic nature. Also, its good distribution in Al matrix restricts Al expansion.
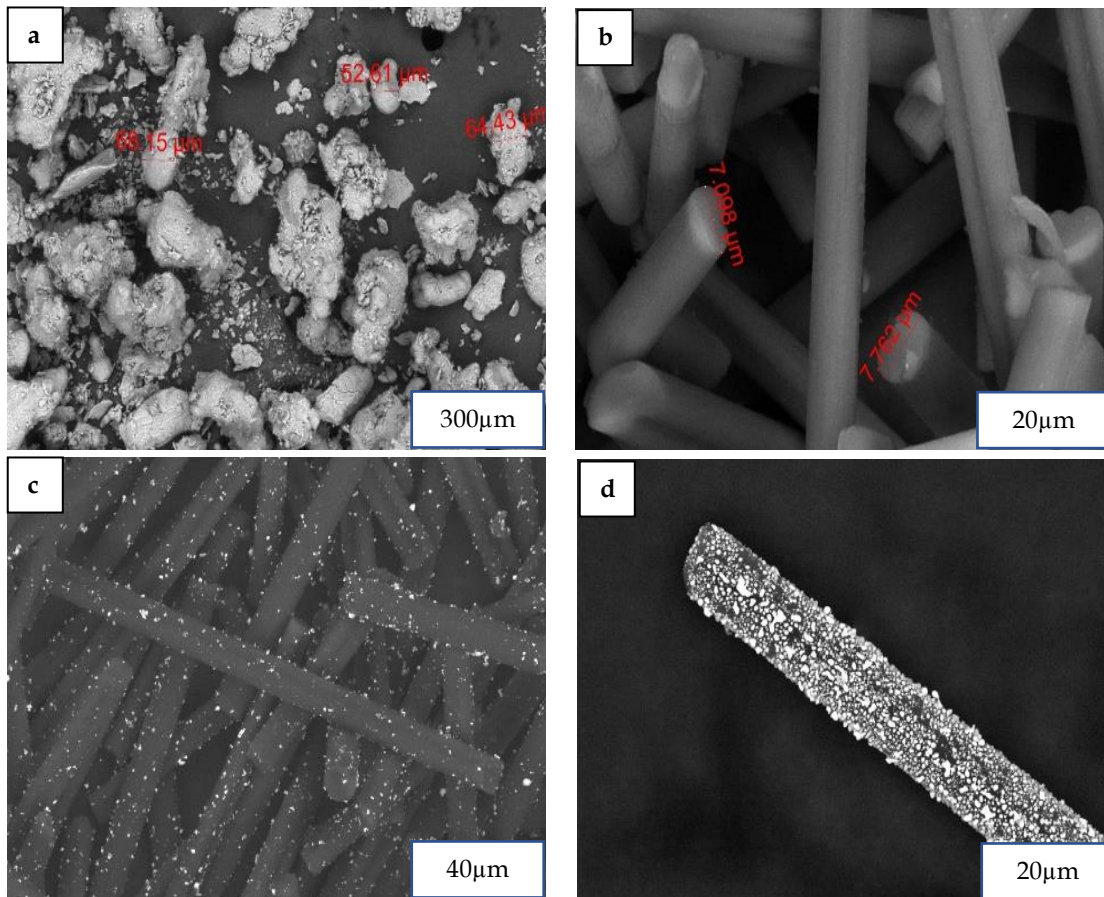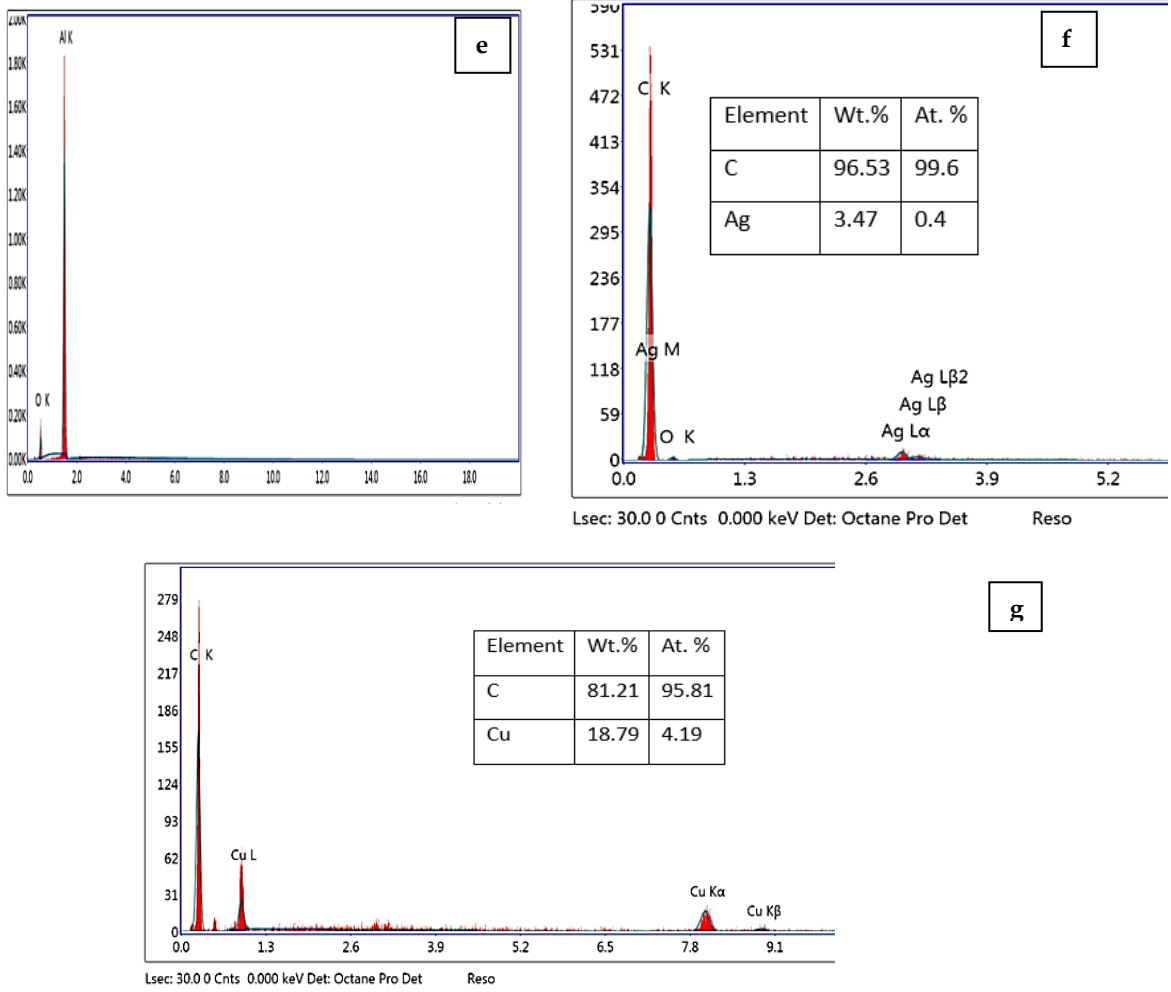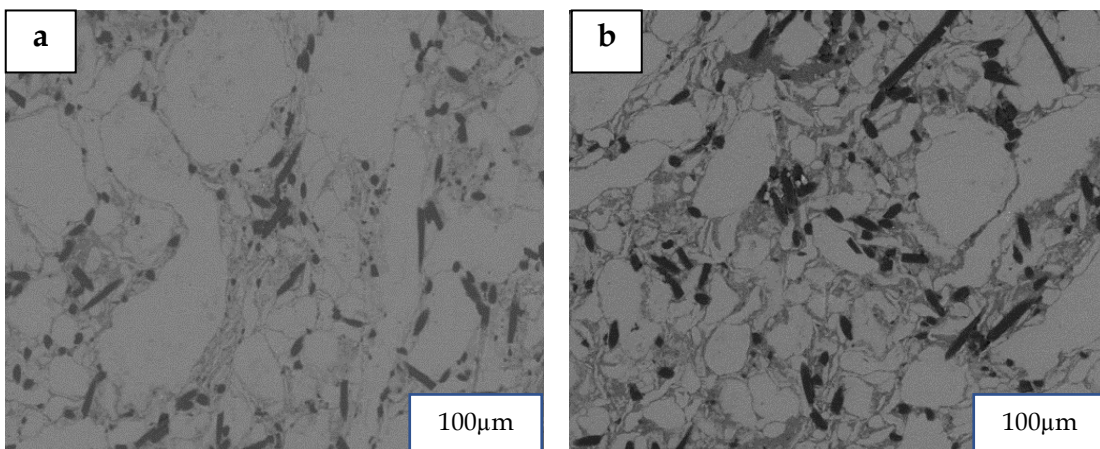
Figure 1: Microstructure of (a) Al powders, (b) CF powders, (c) Activated CF (d) Coated CF, EDAX of (e) Al powders, (f) Activated CF, and (g) Coated CF.
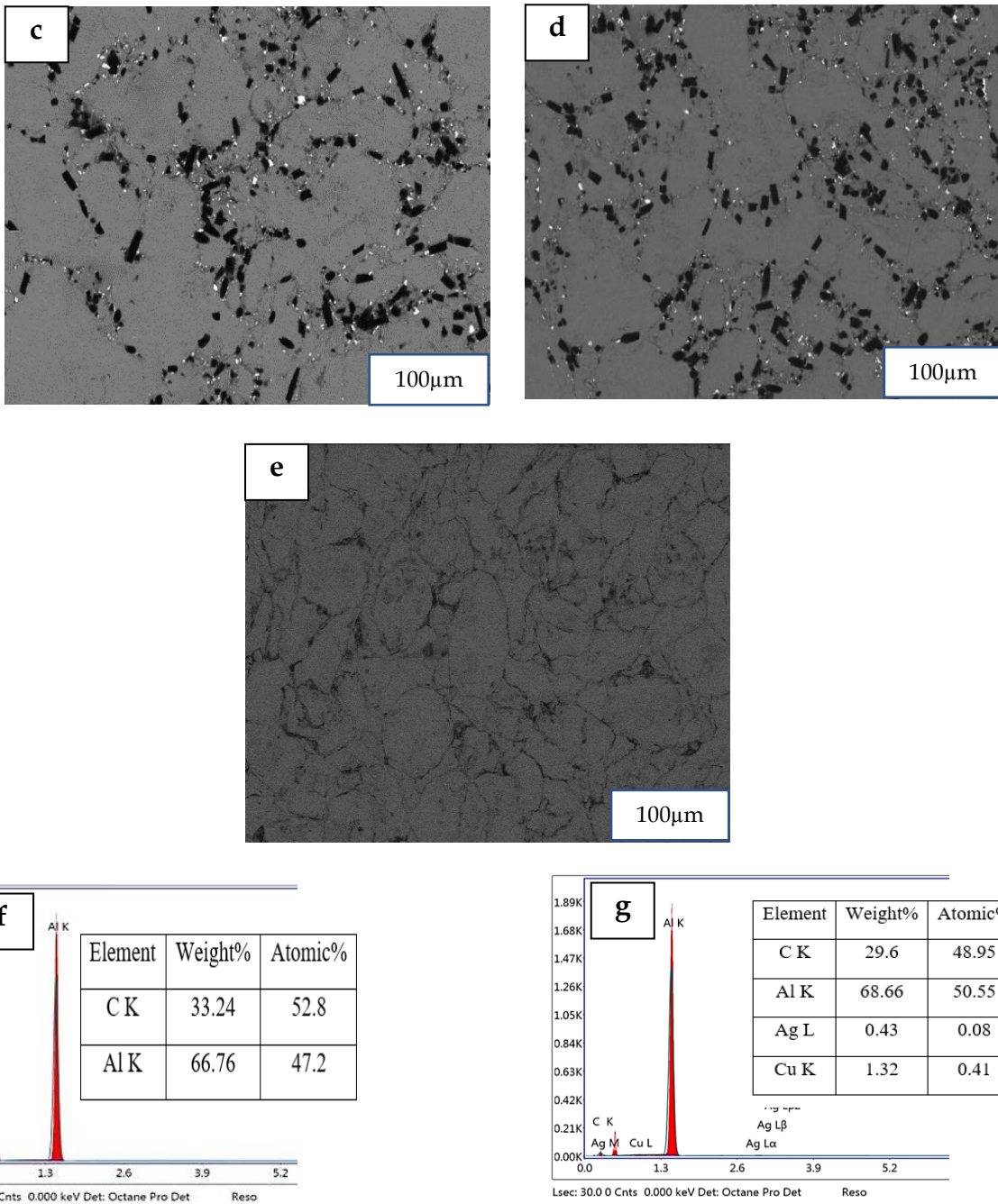
Figure 2: Sem microstructure of CF/Al composites (a) 5 wt.% CF/Al, (b) 15 wt.% CF/Al, (c) 5 wt.% Cu-coated CF/Al, (d) 15 wt.% Cu-coated CF/Al composite, (e) pure sample, and EDAX of 10 wt.%CF/Al (f) Uncoated sample, and (g) Coated sample.
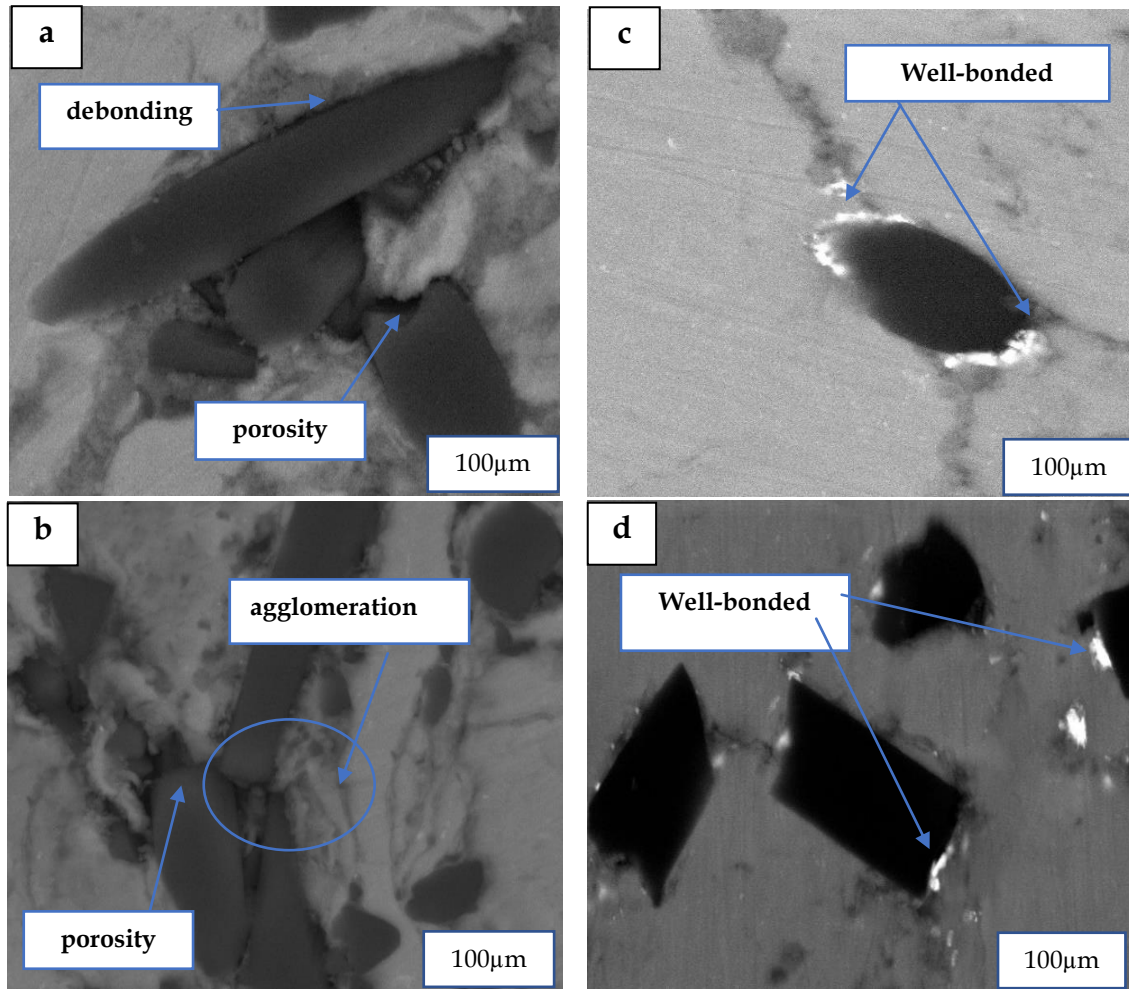
Figure 3: *SEM images of the interface of (a) 5 wt.% CF/Al, (b) 15 wt.% CF/Al, (c) 5 wt.% Cu-coated CF/Al, and (d) 15 wt.% Cu-coated CF/Al composite.*

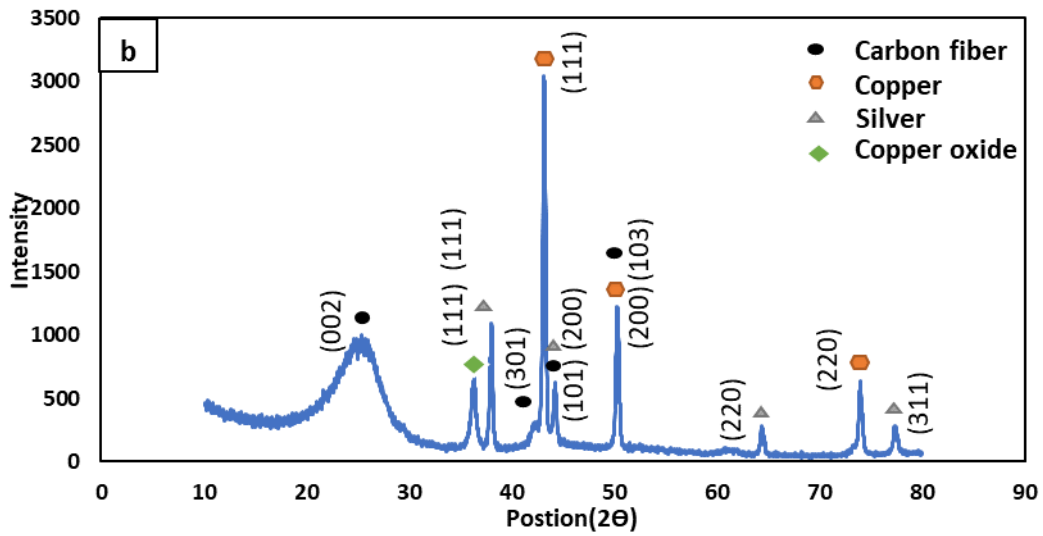| Table1.Crystallite size of composites.							
	Neat	Uncoated fiber			Coated fiber		
The weight percentage of CF	0	5	10	15	5	10	15
Size(nm)	40.02	39.28	36.52	33.89	3.58	34.99	32.34
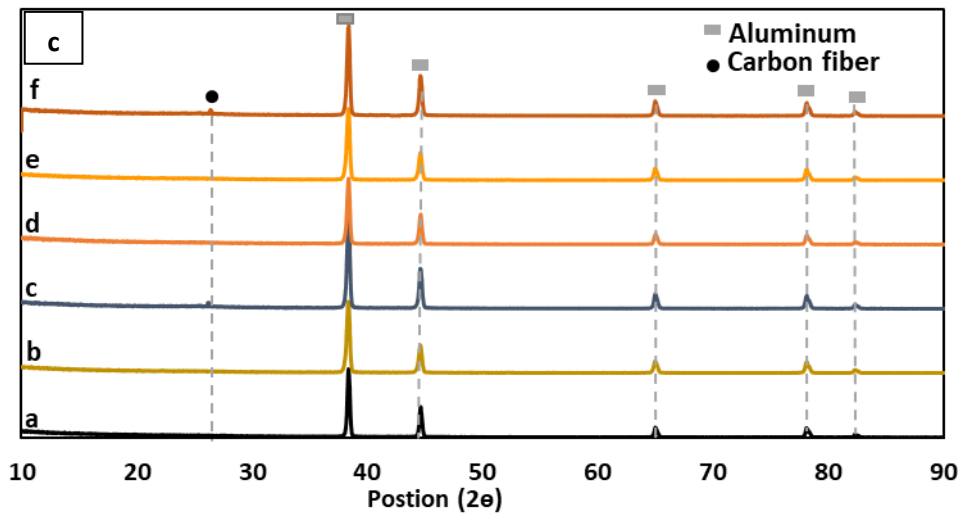
Figure 4: XRD of (a) Al powders, (b) Coated CF powders, and (c) CF/Al composites; a) 5 wt.% CF/Al, (b) 10 wt.% CF/Al, (c) 15 wt.% CF/Al, (d) 5 wt.% Cu-coated CF/Al, (e) 10 wt.% Cu-coated CF/Al, and (f) 15 wt.% Cu-coated CF/Al.
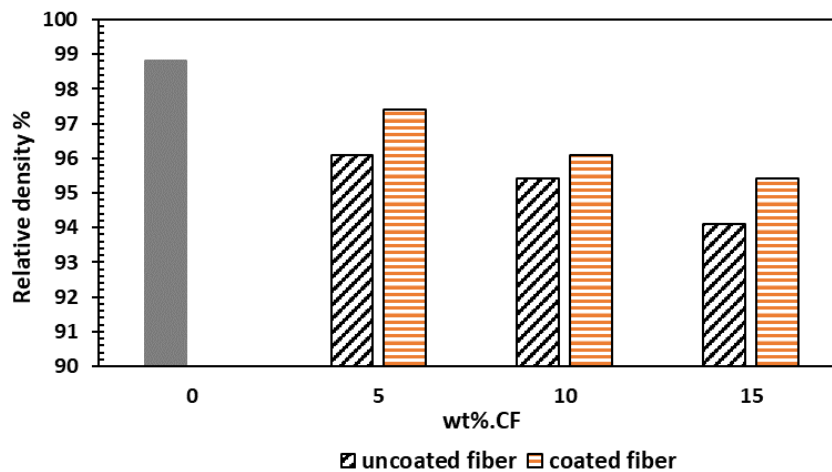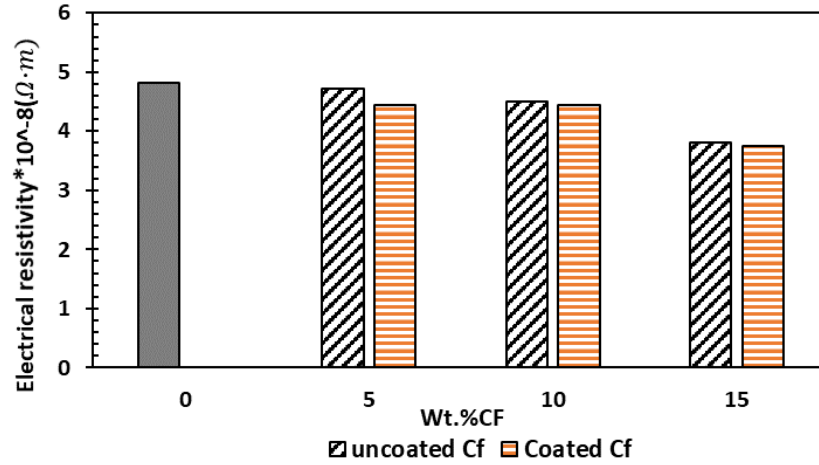

Figure 5: Relative density of CF/Al composites.
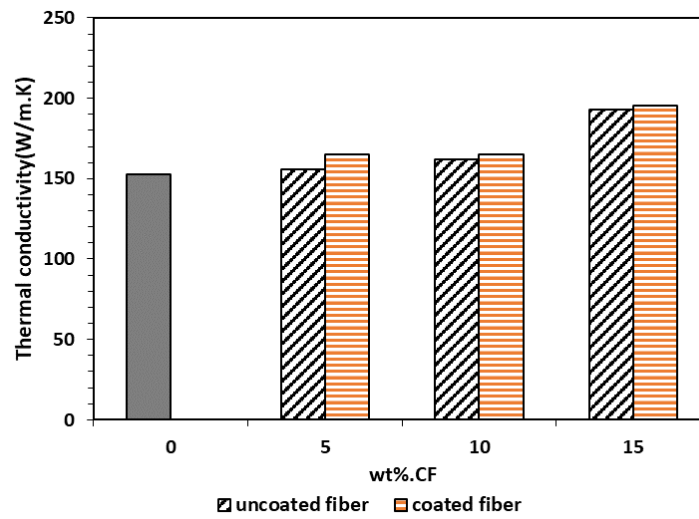
Figure 6: *Electrical resistivity of CF/Al composites.*

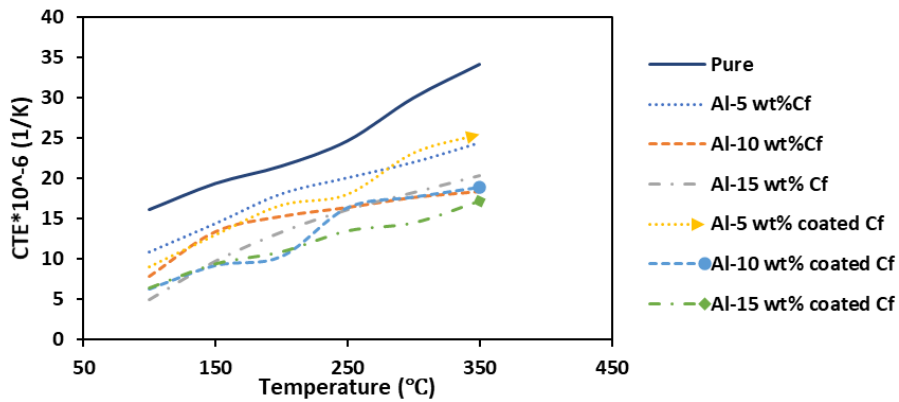**Figure 7:** *Thermal conductivity of CF/Al composites.*

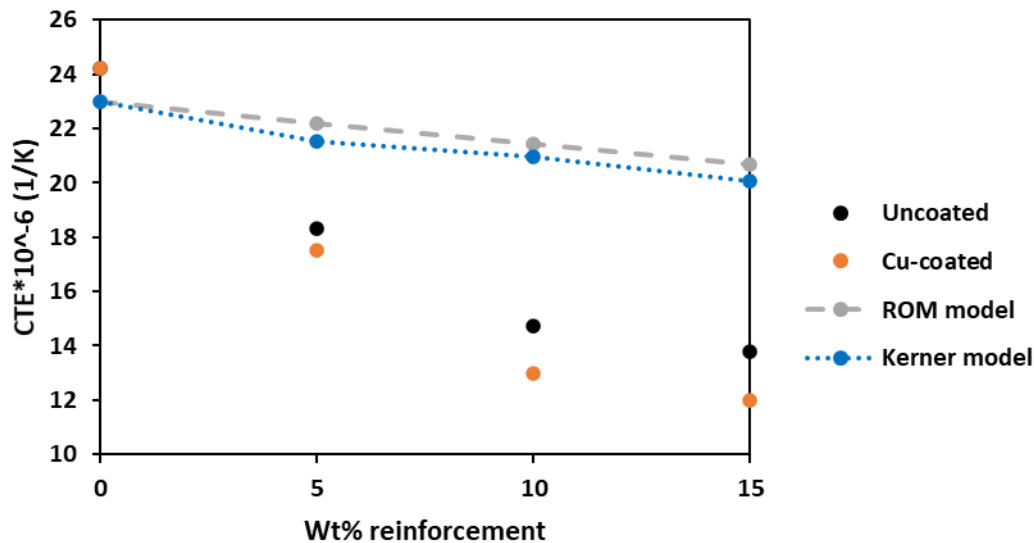**Figure 8:** *CTE of CF/Al composites versus temperature.*

Figure 9: *Comparison between experimental and predicted CTE versus CF content in the temperature range of 100–350 ℃.*

4. CONCLUSION

In conclusion, uncoated and Cu-coated CF/Al composites were fabricated using the hot-pressing technique. The present study focused on the effects of reinforcement and electroless coating process on the microstructure, electrical and thermal properties of CF/Al composites, and the subsequent conclusions are as follows:

1. CF particles are uniformly distributed in Al composites with and without Cu coating. Electroless Cu coating improved the microstructure of interface and bonding between the two constituents of composites.
2. XRD showed that CF refined crystallite size of the Al matrix and neither AL4C3 nor Al2Cu was observed in the structure.
3. Although the relative density decreased with an increase in CF fraction, high dense composites could be obtained from our fabrication technique.
4. The electrical and thermal conductivities of composites improved when CF was added to the Al matrix. On the other hand, the coated composites had much higher conductivity values than uncoated composites.
5. CTE increased linearly with temperature increase and decreased with CF addition. Coated composites were more efficient to inhibit the thermal expansion of the Al matrix.
6. The present investigation showed that the microstructures, electrical and thermal properties of CF /Al composites fabricated by the hot-pressing process could be improved by CF surface modification with Cu

REFERENCES

[1] J.K. Chen, I.S. Huang, Thermal properties of aluminum–graphite composites by powder metallurgy, Compos. Part B Eng., vol.44, (2013) ,pp.698–703.

[2] A.T. Miranda, L. Bolzoni, N. Barekar, Y. Huang, J. Shin, S.-H. Ko, B.J. McKay, Processing, structure and thermal conductivity correlation in carbon fibre reinforced aluminium metal matrix composites, Mater. Des., vol.156, (2018) ,pp.329–339.

[3] J.-D. Mathias, P.-M. Geffroy, J.-F. Silvain, Architectural optimization for microelectronic packaging, Appl. Therm. Eng., vol.29, (2009) ,pp.2391–2395.

[4] K. Shirvanimoghaddam, S.U. Hamim, M.K. Akbari, S.M. Fakhrhoseini, H. Khayyam, A.H. Pakseresht, E. Ghasali, M. Zabet, K.S. Munir, S. Jia, Carbon fiber reinforced metal matrix composites: Fabrication processes and properties, Compos. Part A Appl. Sci. Manuf., vol.92, (2017) ,pp.70–96.

[5] T. Fei, Y.U. Kun, L.U.O. Jie, H. Fang, C. Shi, Y. Dai, H. Xiong, Microstructures and properties of Al–50% SiC composites for electronic packaging applications, Trans. Nonferrous Met. Soc. China., vol.26, (2016) ,pp.2647–2652.

[6] J.M. Molina, J. Narciso, L. Weber, A. Mortensen, E. Louis, Thermal conductivity of Al–SiC composites with monomodal and bimodal particle size distribution, Mater. Sci. Eng. A., vol.480, (2008) ,pp.483–488.

[7] P.W. Ruch, O. Beffort, S. Kleiner, L. Weber, P.J. Uggowitzer, Selective interfacial bonding in Al (Si)–diamond composites and its effect on thermal conductivity, Compos. Sci. Technol., vol.66, (2006) ,pp.2677–2685.

[8] J. Cho, K.E. Goodson, Thermal transport: cool electronics, NatMa., vol.14, (2015) ,pp.136–137.

[9] Y. Huang, Y. Su, S. Li, Q. Ouyang, G. Zhang, L. Zhang, D. Zhang, Fabrication of graphite film/aluminum composites by vacuum hot pressing: process optimization and thermal conductivity, Compos. Part B Eng., vol.107, (2016) ,pp.43–50.

[10] L.G. Hou, R.Z. Wu, X.D. Wang, J.H. Zhang, M.L. Zhang, A.P. Dong, B.D. Sun, Microstructure, mechanical properties and thermal conductivity of the short carbon fiber reinforced magnesium matrix composites, J. Alloys Compd., vol.695, (2017) ,pp.2820–2826.

[11] J.M. Ullbrand, J.M. Córdoba, J. Tamayo-Ariztondo, M.R. Elizalde, M. Nygren, J.M. Molina-Aldareguia, M. Odén, Thermomechanical properties of copper–carbon nanofibre composites prepared by spark plasma sintering and hot pressing, Compos. Sci. Technol., vol.70, (2010) ,pp.2263–2268.

[12] S. Mallik, N. Ekere, C. Best, R. Bhatti, Investigation of thermal management materials for automotive electronic control units, Appl. Therm. Eng., vol.31, (2011) ,pp.355–362.

[13] X. Qu, L. Zhang, W.U. Mao, S. Ren, Review of metal matrix composites with high thermal conductivity for thermal management applications, Prog. Nat. Sci. Mater. Int., vol.21, (2011) ,pp.189–197.

[14] R. Prieto, J.M. Molina, J. Narciso, E. Louis, Fabrication and properties of graphite flakes/metal composites for thermal management applications, Scr. Mater., vol.59, (2008) ,pp.11–14.

[15] M. Lee, Y. Choi, K. Sugio, K. Matsugi, G. Sasaki, Effect of aluminum carbide on thermal conductivity of the unidirectional CF/Al composites fabricated by low pressure infiltration process, Compos. Sci. Technol., vol.97, (2014) ,pp.1–5.

[16] M. Baghi, B. Niroumand, R. Emadi, Fabrication and characterization of squeeze cast A413-CSF composites, J. Alloys Compd., vol.710, (2017) ,pp.29–36.

[17] G. Lalet, H. Kurita, T. Miyazaki, A. Kawasaki, J.-F. Silvain, Thermomechanical stability of a carbon fiber-reinforced aluminum matrix composite fabricated by spark plasma sintering in various pulse conditions, Mater. Lett., vol.130, (2014) ,pp.32–35.

[18] H. Kurita, E. Feuillet, T. Guillemet, J.-M. Heintz, A. Kawasaki, J.-F. Silvain, Simple fabrication and characterization of discontinuous carbon fiber reinforced aluminum matrix composite for lightweight heat sink applications, Acta Metall. Sin. (English Lett., vol.27, (2014) ,pp.714–722.

[19] J.-F. Silvain, A. Veillère, Y. Lu, Copper-carbon and aluminum-carbon composites fabricated by powder metallurgy processes, in: J. Phys. Conf. Ser., IOP Publishing, 2014: p. 12015.

[20] E. Hajjari, M. Divandari, A.R. Mirhabibi, The effect of applied pressure on fracture surface and tensile properties of nickel coated continuous carbon fiber reinforced aluminum composites fabricated by squeeze casting, Mater. Des., vol.31, (2010) ,pp.2381–2386.

[21] A. Urena, J. Rams, M.D. Escalera, M. Sanchez, Characterization of interfacial mechanical properties in carbon fiber/aluminium matrix composites by the nanoindentation technique, Compos. Sci. Technol., vol.65, (2005) ,pp.2025–2038.

[22] Y. Huang, Q. Ouyang, Q. Guo, X. Guo, G. Zhang, D. Zhang, Graphite film/aluminum laminate composites with ultrahigh thermal conductivity for thermal management applications, Mater. Des., vol.90, (2016) ,pp.508–515.

[23] H. Kurita, T. Miyazaki, A. Kawasaki, Y. Lu, J.-F. Silvain, Interfacial microstructure of graphite flake reinforced aluminum matrix composites fabricated via hot pressing, Compos. Part A Appl. Sci. Manuf., vol.73, (2015) ,pp.125–131.

[24] K. Landry, S. Kalogeropoulou, N. Eustathopoulos, Wettability of carbon by aluminum and aluminum alloys, Mater. Sci. Eng. A., vol.254, (1998) ,pp.99–111.

[25] Y. Huang, Q. Ouyang, D. Zhang, J. Zhu, R. Li, H. Yu, Carbon materials reinforced aluminum composites: a review, Acta Metall. Sin. (English Lett., vol.27, (2014) ,pp.775–786.

[26] M.A. Awotunde, A.O. Adegbenjo, B.A. Obadele, M. Okoro, B.M. Shongwe, P.A. Olubambi, Influence of sintering methods on the mechanical properties of aluminium nanocomposites reinforced with carbonaceous compounds: A review, J. Mater. Res. Technol., (2019).

[27] A.A. Baker, M.C. Shipman, P.W. Jackson, The short-term compatibility of carbon fibres with aluminium, Fibre Sci. Technol., vol.5, (1972) ,pp.213–218.

[28] H. Nayeb-Hashemi, J. Seyyedi, Study of the interface and its effect on mechanical properties of continuous graphite fiber-reinforced 201 aluminum, Metall. Trans. A., vol.20, (1989) ,pp.727–739.

[29] A.A. Baker, Carbon fibre reinforced metals—a review of the current technology, Mater. Sci. Eng., vol.17, (1975) ,pp.177–208.

[30] S.J. Baker, W. Bonfield, Fracture of aluminium-coated carbon fibres, J. Mater. Sci., vol.13, (1978) ,pp.1329–1334.

[31] S.C. Tjong, Recent progress in the development and properties of novel metal matrix nanocomposites reinforced with carbon nanotubes and graphene nanosheets, Mater. Sci. Eng. R Reports., vol.74, (2013) ,pp.281–350.

[32] Z. Tan, Z. Li, G. Fan, Q. Guo, X. Kai, G. Ji, L. Zhang, D. Zhang, Enhanced thermal conductivity in diamond/aluminum composites with a tungsten interface nanolayer, Mater. Des., vol.47, (2013) ,pp.160–166.

[33] A. Daoud, Microstructure and tensile properties of 2014 Al alloy reinforced with continuous carbon fibers manufactured by gas pressure infiltration, Mater. Sci. Eng. A., vol.391, (2005) ,pp.114–120.

[34] J. Hashim, L. Looney, M.S.J. Hashmi, The wettability of SiC particles by molten aluminium alloy, J. Mater. Process. Technol., vol.119, (2001) ,pp.324–328.

[35] S. Ghosh, Electroless copper deposition: A critical review, Thin Solid Films., vol.669, (2019) ,pp.641–658.

[36] J. Sudagar, J. Lian, W. Sha, Electroless nickel, alloy, composite and nano coatings–A critical review, J. Alloys Compd., vol.571, (2013) ,pp.183–204.

[37] Y. Mu, G. Yao, G. Zu, Z. Cao, Influence of strain amplitude on damping property of aluminum foams reinforced with copper-coated carbon fibers, Mater. Des., vol.31, (2010) ,pp.4423–4426.

[38] B.B. Singh, M. Balasubramanian, Processing and properties of copper-coated carbon fibre reinforced aluminium alloy composites, J. Mater. Process. Technol., vol.209, (2009) ,pp.2104–2110.

[39] W.M. Daoush, T.S. Alkhuraiji, M.A. Khamis, T.S. Albogmy, Microstructure and electrical properties of carbon short fiber reinforced copper composites fabricated by electroless deposition followed by powder metallurgy process, Carbon Lett., (2019) ,pp.1–12.

[40] C. Shi, J. Lei, S. Zhou, X. Dai, L.-C. Zhang, Microstructure and mechanical properties of carbon fibers strengthened Ni-based coatings by laser cladding: The effect of carbon fiber contents, J. Alloys Compd., vol.744, (2018) ,pp.146–155.

[41] J. Rams, A. Urena, M.D. Escalera, M. Sanchez, Electroless nickel coated short carbon fibres in aluminium matrix composites, Compos. Part A Appl. Sci. Manuf., vol.38, (2007) ,pp.566–575.

[42] G. Jiang, L. Diao, K. Kuang, Advanced thermal management materials, Springer Science & Business Media, 2012.

[43] S.-I. Oh, J.-Y. Lim, Y.-C. Kim, J. Yoon, G.-H. Kim, J. Lee, Y.-M. Sung, J.-H. Han, Fabrication of carbon nanofiber reinforced aluminum alloy nanocomposites by a liquid process, J. Alloys Compd., vol.542, (2012) ,pp.111–117.

[44] T. Liu, X. He, L. Zhang, Q. Liu, X. Qu, Fabrication and thermal conductivity of short graphite fiber/Al composites by vacuum pressure infiltration, J. Compos. Mater., vol.48, (2014) ,pp.2207–2214.

[45] B.T.S. AL-Mosawi, D. Wexler, A. Calka, Characterization and Properties of Aluminium Reinforced Milled Carbon Fibres Composites Synthesized by Uniball Milling and Uniaxial Hot Pressing, Met. Mater. Int., (2020) ,pp.1–24.

[46] K. Kallip, N.K. Babu, K.A. AlOgab, L. Kollo, X. Maeder, Y. Arroyo, M. Leparoux, Microstructure and mechanical properties of near net shaped aluminium/alumina nanocomposites fabricated by powder metallurgy, J. Alloys Compd., vol.714, (2017) ,pp.133–143.

[47] H. Kurita, M. Estili, H. Kwon, T. Miyazaki, W. Zhou, J.-F. Silvain, A. Kawasaki, Load-bearing contribution of multi-walled carbon nanotubes on tensile response of aluminum, Compos. Part A Appl. Sci. Manuf., vol.68, (2015) ,pp.133–139.

[48] Z. Cai, C. Zhang, R. Wang, C. Peng, K. Qiu, Y. Feng, Preparation of Al–Si alloys by a rapid solidification and powder metallurgy route, Mater. Des., vol.87, (2015) ,pp.996–1002.

[49] A. Urena, J. Rams, M.D. Escalera, M. Sanchez, Effect of copper electroless coatings on the interaction between a molten Al–Si–Mg alloy and coated short carbon fibres, Compos. Part A Appl. Sci. Manuf., vol.38, (2007) ,pp.1947–1956.

[50] A. Urena, J. Rams, M. Campo, M. Sanchez, Effect of reinforcement coatings on the dry sliding wear behaviour of aluminium/SiC particles/carbon fibres hybrid composites, Wear., vol.266, (2009) ,pp.1128–1136.

[51] Q. Liu, X.-B. He, S.-B. Ren, T. Liu, Q.-P. Kang, X.-H. Qu, Effect of titanium carbide coating on the microstructure and thermal conductivity of short graphite fiber/copper composites, J. Mater. Sci., vol.48, (2013) ,pp.5810–5817.

[52] A.K. Nittala, Electrical and Mechanical Performance of Aluminum Alloys with Graphite Nanoparticles, (2019).

[53] I. Momohjimoh, N. Saheb, M.A. Hussein, T. Laoui, N. Al-Aqeeli, Electrical conductivity of spark plasma sintered Al2O3–SiC and Al2O3-carbon nanotube nanocomposites, Ceram. Int., (2020).

[54] O. El-Kady, H.M. Yehia, F. Nouh, Preparation and characterization of Cu/(WC-TiC-Co)/graphene nano-composites as a suitable material for heat sink by powder metallurgy method, Int. J. Refract. Met. Hard Mater., vol.79, (2019) ,pp.108–114.

[55] S.E. Shin, H.J. Choi, D. Bae, Electrical and thermal conductivities of aluminum-based composites containing multi-walled carbon nanotubes, J. Compos. Mater., vol.47, (2013) ,pp.2249–2256.

[56] C. Zhang, Z. Cai, R. Wang, C. Peng, K. Qiu, N. Wang, Microstructure and thermal properties of Al/W-coated diamond composites prepared by powder metallurgy, Mater. Des., vol.95, (2016) ,pp.39–47.

[57] S. Ren, X. Shen, C. Guo, N. Liu, J. Zang, X. He, X. Qu, Effect of coating on the microstructure and thermal conductivities of diamond–Cu composites prepared by powder metallurgy, Compos. Sci. Technol., vol.71, (2011) ,pp.1550–1555. http://www.sciencedirect.com/science/article/pii/S0266353811002181.

[58] X. Peng, Y. Huang, X. Han, R. Fan, High volume fraction of copper coated graphite flake\ Nitrogen doped carbon fiber reinforced aluminum matrix composites, J. Alloys Compd., vol.822, (2020) ,pp.153584.

[59] D. Jiang, X. Zhu, J. Yu, Enhanced Thermal Conductivity and Bending Strength of Graphite Flakes/aluminum Composites Via Graphite Surface Modification, J. Wuhan Univ. Technol. Sci. Ed., vol.35, (2020) ,pp.9–15.

[60] O.A.M. Elkady, A. Abu-Oqail, E.M.M. Ewais, M. El-Sheikh, Physico-mechanical and tribological properties of Cu/h-BN nanocomposites synthesized

by PM route, J. Alloys Compd., vol.625, (2015) ,pp.309–317.

[61] Y. Jia, F. Cao, S. Scudino, P. Ma, H. Li, L. Yu, J. Eckert, J. Sun, Microstructure and thermal expansion behavior of spray-deposited Al–50Si, Mater. Des., vol.57, (2014) ,pp.585–591. http://www.sciencedirect.com/science/article/pii/S0261306914000041.

[62] A.L. Geiger, M. Jackson, Low-expansion MMCs boost avionics, Adv. Mater. Process., vol.136, (1989) ,pp.23–30.

[63] P.S. Turner, The problem of thermal-expansion stresses in reinforced plastics, (1942).

[64] A. Fathy, O. El-Kady, Thermal expansion and thermal conductivity characteristics of Cu–Al2O3 nanocomposites, Mater. Des., vol.46, (2013) ,pp.355–359.

[65] Y. ZHANG, G. WU, Interface and thermal expansion of carbon fiber reinforced aluminum matrix composites, Trans. Nonferrous Met. Soc. China., vol.20, (2010) ,pp.2148–2151. http://www.sciencedirect.com/science/article/pii/S1003632609604337.